Journal of Optical Technology

Peculiarities of the acousto-optical field formed during diffraction of dual-mode radiation in uniaxial crystals

V. M. Kotov,[1,2] S. V. Averin,[1] P. I. Kusnetsov,[1] and E. V. Kotov[1]

[1]V. A. Kotel'nikov Institute of Radioengineering and Electronics, Russian Academy of Sciences, Fryazino Branch, Vvedensky Square 1, Fryazino Moscow Region, 141190, Russia
[2]e-mail: vmk277@ire216.msk.su

Received 15 May 2017; Opticheskiĭ Zhurnal **85**, 34–40 (January 2018)

This paper discusses acousto-optic Bragg diffraction in uniaxial crystals when two intrinsic optical modes of the crystal participate in the diffraction. The calculations are based on two crystals widely used in acousto-optics: lithium niobate and paratellurite. It is shown that the character of the acousto-optical field formed in the diffraction orders when optical rays propagate close to the optic axis while a sound wave propagates orthogonally to the optic axis makes it possible to use the resulting field for two-dimensional processing of optical images. The image can be filtered in this case by using both the zeroth and the first diffraction orders. Acousto-optic filters are fabricated from a paratellurite crystal and are used to experimentally show that a two-dimensional contour is discriminated when the image is subjected to optical Fourier processing (fast Fourier transform), using the zeroth and first Bragg orders.

OCIS codes: (070.1060) Acousto-optical signal processing; (070.2615) Frequency filtering; (070.6110) Spatial filtering.

https://doi.org/10.1364/JOT.85.000026

1. INTRODUCTION

The contour of an image is discriminated by a widely practiced method of processing optical images, after which it is recognized (for example, see [1]). The goal of the contour-discrimination operation is to substantially reduce the volume of information to be processed while preserving such important characteristic parameters of the image as its shape and size. These parameters are in many cases quite sufficient to recognize the object.

Acousto-optic (AO) elements are widely used as controllable spatial-frequency filters in order to Fourier-process various optical fields and images [2–7]. In particular, such filters can be used to distinguish one-dimensional [3,4] and two-dimensional contours [5–7]. Later versions are of most interest in practice, since they fully solve the problem of distinguishing the two-dimensional contour of an object.

A typical layout of the optical apparatus for Fourier-processing an image is shown in Fig. 1 [1]. The layout is based on two lenses L_1 and L_2. We assume for simplicity that the lenses have the same focal length F. Input-image plane S_{in} is positioned in front of lens L_1 at the focal length from it. Acousto-optic modulator AOM, which serves the function of filtering spatial frequencies, is positioned behind lens L_1 at the same focal length. An electric signal with frequency f is applied to the modulator. Lens L_2 is positioned behind the modulator at focal length F, and screen S_{out} (the plane of the output image) is positioned behind that at the same length F. A feature of using an AO modulator is that there are two images on the screen, corresponding to two diffraction orders. In our experiments, polarizers P_1 and P_2, which improve the characteristics of the two-dimensional image, were installed in front of AOM and behind it. A two-dimensional contour of the image is formed on the screen in one of the diffraction orders by appropriately choosing the frequency supplied to AOM and the necessary orientation of the modulator and the polarizers. We should point out that, when the ordinary AO diffraction regime is used, it is not possible in general to obtain a two-dimensional contour when only one of the intrinsic optical modes of the crystal participates in the diffraction. This can be done only when both optical modes are involved in the diffraction process. The proposed version of diffraction possesses a number of features that are considered in the next section.

2. THEORY

A vector diagram of the AO diffraction of dual-mode optical radiation is shown in Fig. 2. The initial optical radiation transmitted by light with wave vector **K** is incident on the optical face (XY) of the crystal. Acoustic wave **q** propagates in the Y direction. Plane P_d contains vector **K** and passes through the Y axis. Plane P_d slopes toward optic axis Z by angle α. The orientation of vector **K** is given by angles α and β.

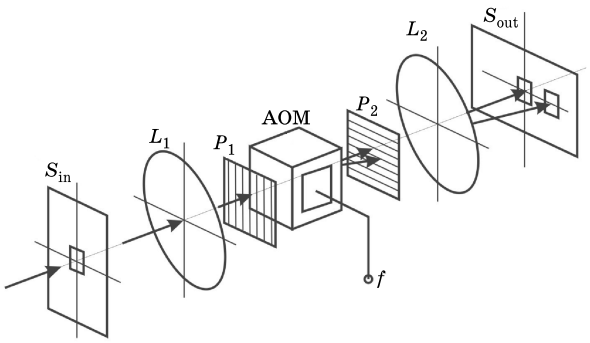

Fig. 1. Optical layout for Fourier-processing a two-dimensional optical image. L_1 and L_2 are lenses, AOM is an AO modulator, P_1 and P_2 are polarizers, S_{in} is the plane of the input image, and S_{out} is the plane of the output image (a screen).

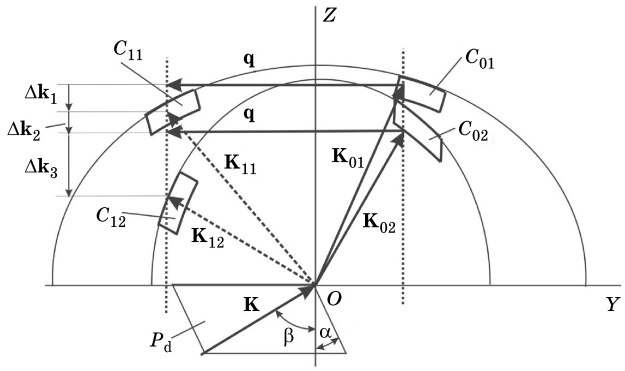

Fig. 2. Vector diagram of AO diffraction of dual-mode optical radiation.

Angle β is defined as the angle between the projection of vector $\mathbf{K}$ onto the ZY plane and the Z axis. Inside the crystal, the incident radiation is represented in the form of two intrinsic modes with wave vectors $\mathbf{K}_{01}$ and $\mathbf{K}_{02}$. The amplitude distributions of these modes over the surfaces of the wave vectors are denoted by C_{01} and C_{02}, which intrinsically carry information concerning the input image in the absence of a sound wave. As a result of diffraction on an acoustic wave with wave vector $\mathbf{q}$, modes $\mathbf{K}_{01}$ and $\mathbf{K}_{02}$ diffract in the direction of modes $\mathbf{K}_{11}$ and $\mathbf{K}_{12}$. The amplitude distributions of the diffracted modes are designated C_{11} and C_{12}, respectively. It is understood that, in general, diffraction is accompanied by detuning Bragg synchronism. Generally speaking, each of the incident modes $\mathbf{K}_{01}$ or $\mathbf{K}_{02}$ diffract at once into the two modes $\mathbf{K}_{11}$ and $\mathbf{K}_{12}$ with different efficiency in this case. Mode $\mathbf{K}_{01}$ diffracts into $\mathbf{K}_{11}$ with synchronism-detuning vector $\Delta\mathbf{k}_1$, $\mathbf{K}_{02}$ diffracts into $\mathbf{K}_{11}$ and $\mathbf{K}_{22}$ with detunings $\Delta\mathbf{k}_2$ and $\Delta\mathbf{k}_3$, respectively. Mode $\mathbf{K}_{01}$ diffracts into $\mathbf{K}_{12}$ with detunings $\Delta\mathbf{k}_1 + \Delta\mathbf{k}_2 + \Delta\mathbf{k}_3$. Modes $\mathbf{K}_{01}$, $\mathbf{K}_{02}$, $\mathbf{K}_{11}$, and $\mathbf{K}_{12}$ are connected with each other via AO interaction. To find the amplitudes C_{01}, C_{02}, C_{11}, and C_{12}, it is necessary to solve the system of differential equations [8,9]

$$
\begin{aligned}
2\frac{dC_{01}}{dz} &= -m_1 C_{11}\exp(-i\Delta\mathbf{k}_1 z) - m_2 C_{12}\exp(i\Delta\mathbf{k}_2 z),\\
2\frac{dC_{02}}{dz} &= -m_3 C_{12}\exp(-i\Delta\mathbf{k}_3 z)\\
&\quad - m_4 C_{11}\exp[-i(\Delta\mathbf{k}_1 + \Delta\mathbf{k}_2 + \Delta\mathbf{k}_3)z],\\
2\frac{dC_{11}}{dz} &= m_1 C_{01}\exp(i\Delta\mathbf{k}_1 z)\\
&\quad + m_4 C_{02}\exp[i(\Delta\mathbf{k}_1 + \Delta\mathbf{k}_2 + \Delta\mathbf{k}_3)z],\\
2\frac{dC_{12}}{dz} &= m_2 C_{01}\exp(-i\Delta\mathbf{k}_2 z) + m_3 C_{02}\exp(i\Delta\mathbf{k}_3 z),
\end{aligned}
\qquad (1)
$$

where C_{01}, C_{02}, C_{11}, and C_{12} are the amplitudes of rays, $\mathbf{K}_{02}$, $\mathbf{K}_{11}$, and $\mathbf{K}_{12}$, respectively; z is the direction along which the AO interaction evolves; Δk_1, Δk_2, and Δk_3 are the moduli of detuning vectors $\Delta\mathbf{k}_1$, $\Delta\mathbf{k}_2$ and $\Delta\mathbf{k}_3$; and $m_{1\text{-}4}$ are the Raman–Nath parameters. These are defined as

$$
m_{1\text{-}4} = 2\pi\sqrt{M_{(1\text{-}4)}P_a(2LH)^{-1}}\lambda^{-1}, \qquad (2)
$$

where λ is the wavelength of the light; L and H are respectively the AO interaction length and the height of the acoustic column; P_a is the power of the sound wave; and $M_{(1\text{-}4)}$ are the AO quality coefficients of the material, known in the literature as the M_2 coefficient (for example, see [8] and [10]). We shall assume for definiteness that the diffraction occurs in the uniaxial negative $LiNbO_3$ crystal, whose principal refractive indices are n_o and n_e. The external wave surface of the crystal then describes the propagation of the ordinary wave, and the internal wave describes that of the extraordinary wave. In this case,

$$
\begin{aligned}
M_1 &= n_o^6 p_{ee}^2(\rho V^3)^{-1}, \qquad M_2 = n_o^6 p_{oe}^2(\rho V^3)^{-1},\\
M_3 &= n_o^6 p_{eo}^2(\rho V^3)^{-1}, \qquad M_4 = n_o^6 p_{oo}^2(\rho V^3)^{-1}.
\end{aligned}
\qquad (3)
$$

Here ρ is the density of the crystal, V is the speed of sound, p_{ee} is the effective photoelasticity coefficient, which describes the diffraction of the extraordinary ray into an extraordinary ray [the (e–e) form of diffraction], p_{oe} describes that of an ordinary ray into an extraordinary ray (o–e). Coefficients p_{eo} and p_{oo} describe diffraction of the forms (e–o) and (o–o), respectively.

To determine the photoelasticity coefficients, it is necessary to know the polarization orientations of the crystal's intrinsic modes. They substantially depend on the orientation of the incident radiation.

Let the orientation of the wave vector $\mathbf{K}$ of the incident radiation be given by angles α and β. The projection of $\mathbf{K}$ onto the X, Y, Z directions will then equal

$$
\begin{aligned}
K_x &= |K|\cos\beta\sin\alpha, \qquad K_y = |K|\sin\beta,\\
K_z &= |K|\cos\beta\cos\alpha.
\end{aligned}
\qquad (4)
$$

Here $|K| = 2\pi/\lambda$. Inside the crystal, the projections K_x and K_y of the refracted rays remain the same because of the law of refraction, while projection K_z varies. They become equal to

$$
K_{z1} = [K_o^2 - (K_x^2 + K_y^2)]^{0.5}
$$

for the ordinary ray, and

$$K_{z2} = K_o[1 - (K_x^2 + K_y^2)K_e^{-2}]^{0.5} \quad (5)$$

for the extraordinary ray.

Here $K_o = 2\pi n_o/\lambda$ and $K_e = 2\pi n_e/\lambda$. The refraction angles η_{io} and η_{ie} of the ordinary and extraordinary rays are then determined from

$$\tan\eta_{io} = K_{z1}^{-1}\sqrt{K_x^2 + K_y^2}, \qquad \tan\eta_{ie} = K_{z2}^{-1}\sqrt{K_x^2 + K_y^2}. \quad (6)$$

It is convenient to write the polarization of the ordinary and extraordinary rays in the form of the column vectors

$$e_{io} = \begin{Bmatrix} \sin\xi_{io} \\ -\cos\xi_{io} \\ 0 \end{Bmatrix}, \qquad e_{ie}\begin{Bmatrix} -\cos\xi_{ie}\cos\eta_{ie} \\ -\sin\xi_{ie}\cos\eta_{ie} \\ \sin\eta_{ie} \end{Bmatrix}, \quad (7)$$

where angles ξ_{io} and ξ_{ie} are determined from

$$\tan\xi_{io} = \tan\xi_{ie} = K_x^{-1}K_y. \quad (8)$$

The polarizations of the diffracted rays are described by the same expressions as in Eqs. (7), except that the angles included in these equations will be different. Here angles ξ_{io} and ξ_{ie} will be replaced by ξ_{do} and ξ_{de}, determined by

$$\tan\xi_{do} = \tan\xi_{de} = K_x^{-1}(K_y - q). \quad (9)$$

Here q is the length of the wave vector of sound. The other pair of angles η_{do} and η_{de} is determined from

$$\tan\eta_{do} = K_{z1d}^{-1}\sqrt{K_x^2 + (K_y - q)^2},$$
$$\tan\eta_{de} = K_{z2d}^{-1}\sqrt{K_x^2 + (K_y - q)^2}, \quad (10)$$

where

$$K_{z1d} = \sqrt{K_0^2 - [K_x^2 + (K_y - q)^2]},$$
$$K_{z2d} = K_0\sqrt{1 - K_e^{-2}[K_x^2 + (K_y - q)^2]}.$$

The moduli of the wave vectors of the synchronism detunings are defined as

$$\Delta k_1 = \sqrt{K_o^2 - (K_x^2 + K_y^2)} - \sqrt{K_o^2 - [K_x^2 + (K_y - q)^2]},$$
$$\Delta k_2 = \sqrt{K_o^2 - (K_x^2 + K_y^2)} - K_0\sqrt{1 - K_e^{-2}[K_x^2 + (K_y - q)^2]},$$
$$\Delta k_3 = K_o\sqrt{1 - K_e^{-2}(K_x^2 + K_y^2)} - K_o\sqrt{1 - K_e^{-2}[K_x^2 + (K_y - q)^2]}. \quad (11)$$

We assume that diffraction occurs on the transverse acoustic wave that propagates along the Y direction, with its shift direction along X. The photoelasticity constants are then computed according to the technique described in [11] and in this case equal

$$p_{oe} = 0.5[p_{41}\sin\eta_{de}\sin\xi_{io} + p_{66}\cos\eta_{de}\cos(\xi_{io} + \xi_{de})], p_{oo} = -0.5p_{66}\sin(\xi_{io} + \xi_{do}), p_{ee} = 0.5[p_{66}\cos\eta_{ie}\cos\eta_{de}\sin(\xi_{ie} + \xi_{de}) - p_{41}(\sin\eta_{ie}\cos\eta_{de}\cos\xi_{de} + \sin\eta_{de}\cos\xi_{ie}\cos\eta_{ie})], p_{eo} = 0.5[p_{41}\sin\eta_{de}\sin\xi_{do} + p_{66}\cos\eta_{ie}\cos(\xi_{ie} + \xi_{do})]. \quad (12)$$

Here p_{41} and p_{66} are the components of the matrix of photoelastic coefficients.

We assume that the polarization of the incident optical radiation is oriented along X. The polarization is determined by the orientation of polarizer P_1 (see Fig. 1). The polarization directions of the refracted rays inside the crystal will be determined by the principal plane [12]—i.e., by the plane that contains the wave vector of the light and the optic axis of the crystal. The polarization of the ordinary ray is orthogonal to the principal plane, and that of the extraordinary ray lies in the principal plane and is orthogonal to the wave vector of the light. Of course, the orientation of the principal plane, and hence the polarization directions, will vary as the angles α and β vary. This causes the field to be redistributed between the refracted rays. Let the output polarizer P_2 be oriented at an angle ψ to the input polarizer. The field amplitudes of the refracted rays will then be $C_{01} = C\sin\psi$ and $C_{02} = C\cos\psi$, where C is the amplitude of the incident wave, while the system of Eqs. (1) needs to be solved with boundary conditions $C_{01} = \sin\psi/2^{0.5}$, $C_{02} = \cos\psi/2^{0.5}$, and $C_{11} = C_{12} = 0$ when $z = 0$. Solving Eq. (1), we determine the field amplitude in the zeroth diffraction order after polarizer P_2:

$$A_0 = \sqrt{A_1^2 + A_2^2 + 2A_1A_2\cos(\varphi_1 - \varphi_2)}. \quad (13)$$

Here A_0 is the total field amplitude of the zeroth diffraction order after the polarizer; A_1 and A_2 are the amplitudes of the intrinsic modes, which form the first order,

$$A_1 = C_{01}\sin(\psi - \xi_{io})(\sqrt{2})^{-1},$$
$$A_2 = C_{02}\cos(\psi - \xi_{id})(\sqrt{2})^{-1}; \quad (14)$$

and the phase increment between the intrinsic modes is

$$\varphi_1 - \varphi_2 = 2\pi l_{kr}[n_2(\cos\eta_{ie})^{-1} - n_o(\cos\eta_{io})^{-1}]\lambda^{-1},$$
$$n_2 = n_o n_e\left(\sqrt{n_o^2\sin^2\eta_{ie} + n_e^2\cos^2\eta_{ie}}\right)^{-1}, \quad (15)$$

where l_{kr} is the length of the crystal along Z.

As an example, Fig. 3 shows the results of calculating the field formed in the zeroth diffraction order after polarizer P_2 as a result of AO diffraction in the $LiNbO_3$ [Fig. 3(a)] and TeO_2 crystals [Fig. 3(b)]. For $LiNbO_3$, the calculations were done with the following parameters: $\lambda = 0.63$ μm, $n_o = 2.286$, $n_e = 2.202$, $l_{kr} = 1$ cm, $L = 0.6$ cm, $H = 0.4$ cm, $P_a = 60$ W, $f = 100$ MHz, $\rho = 4.7\text{g/cm}^3$, $V = 3840$ m/s, $p_{41} = -0.151$, $p_{66} = -0.053$ and $\psi = 50°$. The crystal's physical parameters are taken from [13]. Angles α and β are measured from the center of the image, with the center being displaced 0.5° downward and 0.5° to the left in angular space

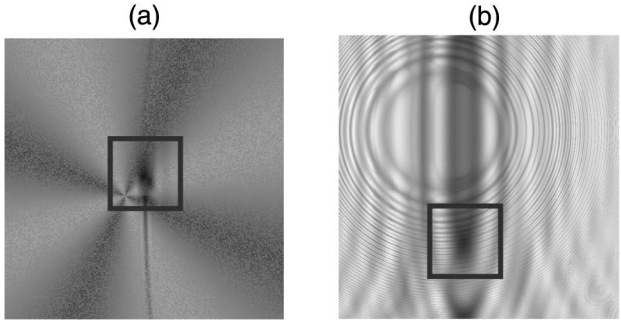

Fig. 3. Acousto-optic fields of zeroth diffraction order, formed as a result of the diffraction of light in (a) $LiNbO_3$ and (b) TeO_2 crystals.

from the crystal's optic axis. This is done so that the working region of the pattern, outlined by a square, is in the center. It can be seen that the AO field as a whole is fairly inhomogeneous. Here a conoscopic pattern is observed as the cruciform field distribution that characterizes the interference pattern that shows up when light propagates close to the crystal's optic axis in crossed polarizers [12,14]. The working region designated on the overall pattern makes it possible to discriminate the two-dimensional contour of the optical image. The size of this entire image is $10° \times 10°$, and that of the working region is about $2° \times 2°$.

Figure 3(b) shows the AO field formed as a result of diffraction in the uniaxial TeO_2 crystal, which possesses gyrotropy. The wave surfaces in the crystal turn out to be more complicated—in the form of $2\pi n_1 \lambda^{-1}$ and $2\pi n_2 \lambda^{-1}$, where n_1 and n_2 are the refractive indices of the gyrotropic crystal [9]:

$$n_{1,2}^2 = (1 + \tan^2\eta)[n_o^{-2} + 0.5\tan^2\eta(n_o^{-2} + n_e^{-2}) \pm 0.5\sqrt{0.5\tan^4\eta(n_o^{-2} - n_e^{-2})^2 + 4G_{33}^2}], \quad (16)$$

where η is the angle between the optic axis Z of the crystal and the direction of the wave vector of the light, n_o and n_e are the principal refractive indices of the crystal, and G_{33} is a component of the pseudotensor of gyration. It is much easier to compute the effective photoelasticity constants of diffraction in the TeO_2. The intrinsic waves of a gyrotropic crystal are circularly polarized when light propagates close to the optic axis. The polarization of the waves is independent of the orientation of the principal plane. The same system of differential Eqs. (1), combined with Eqs. (2), (3), and (12), is used to describe the AO diffraction of dual-mode radiation in TeO_2. Assuming that the light propagates close to the [001] optic axis, while diffraction occurs on the transverse acoustic wave propagating along [110] with displacement along $[1\bar{1}0]$, the effective photoelasticity constants will be

$$p_{eo} = p_{oe} = 0.5(p_{11} - p_{12}),$$
$$p_{oo} = p_{ee} = 0.5p_{eo}. \quad (17)$$

Here p_{11} and p_{12} are the elements of the photoelasticity matrix of TeO_2. These equations are based on [8] and [15]. It is easy to derive from this that the effective photoelasticity constants are independent of angles α and β.

To compute the absolute values Δk of the detuning vectors, it is necessary to use the model of wave vectors described in terms of projections k_x, k_y, and k_z in the following form:

$$k_z^4(k_o^{-4} - [\lambda(2\pi)^{-1}]^4 G_{33}^3) + (k_x^2 + k_y^2)(k_0^{-2} + k_e^{-2})(k_z^2 k_o^{-2} - 1) + k_o^{-2}k_e^{-2}(k_x^2 + k_y^2)^2 - 2k_0^{-2}k_z^2 + 1 = 0. \quad (18)$$

We should point out that detuning vectors Δk mainly depend on AO diffraction in TeO_2; that is, they are chiefly responsible for the dependence of the amplitudes C_{01}–C_{12} on angles α and β.

The calculated diffraction field [Fig. 3(b)] obtained in TeO_2 was computed with the following parameters: $\lambda = 0.63$ μm, $n_o = 2.26$, $n_e = 2.41$, $G_{33} = 2.62 \times 10^{-5}$, $L = 0.6$ cm, $H = 0.4$ cm, $V = 617$ m/s, $f = 28$ MHz, $\rho = 6$ g/cm^3, $0.5(p_{11} - p_{12}) = 0.12$, $P_a = 1$ W, and $\psi = 70°$. It can be seen that the AO field, as before, is inhomogeneous. The conoscopic pattern is observed in the form of a ring, which shows up when linearly polarized light propagates close to the optic axis of a uniaxial gyrotropic crystal at whose output a polarizer is located. The overall size of the image is $10° \times 10°$. The working region is distinguished on the figure by a $2° \times 2°$ square. The overall pattern is displaced in angular space to make it fairly easy to estimate the position of the working region relative to the center of the circle. The center coincides with the direction of the optic axis of the crystal.

The regions outlined in Fig. 3 make it possible to obtain two-dimensional contours of the image. The results of processing with a fast Fourier transformation (FFT) using the outlined regions are shown in Fig. 4. Here Fig. 4(a) shows the input images in the form of a circle and a rectangle, and Fig. 4(b) shows the images after FFT processing. It can be seen in

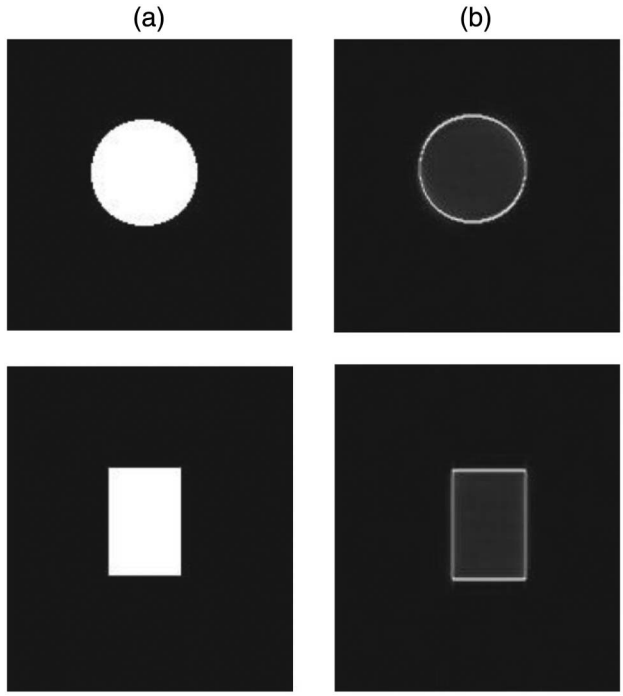

Fig. 4. (a) Initial images and (b) their contours after being processed using the fast Fourier transform.

Fig. 4(b) that the contours of the original images from Fig. 4(a) are clearly expressed. In other words, the use of an AO cell as a spatial-frequency filter with the AO field distribution in the form of the outlined sections in Fig. 3 forms a two-dimensional contour of the image in optical Fourier-processing systems.

Even though the character of the field distribution is different in the outlined regions, the result of the FFT processing is the same: A distinctly expressed two-dimensional contour of the image is formed in both cases.

Based on these theoretical studies, it can be concluded that the AO diffraction of dual-mode optical radiation forms a strongly inhomogeneous diffraction field, individual sections of which make it possible to discriminate a two-dimensional contour of the optical image. The resulting field varies, depending on the frequency and power of the sound, as well as on the positions of the input and output polarizers. We should point out in passing that, generally speaking, other sections of the field can be distinguished that manifest definite two-dimensionality. However, the discriminated sections need to be verified in each case by using them directly as filters in the FFT processing of images.

We should add to what has been said that sections suitable for processing can be found not only in the zeroth order but also in the first diffraction order. All this offers opportunities of using dual-mode diffraction for two-dimensional image processing.

3. EXPERIMENT AND DISCUSSION OF THE EXPERIMENTAL RESULTS

Experiments were carried out to check the theoretical results. The optical layout of the experimental apparatus completely conforms to the diagram in Fig. 1. A 1 mm × 1.5 mm rectangular aperture uniformly illuminated by the wide beam of a He–Ne laser ($\lambda = 0.63$ μm) was chosen as the image to be processed. A Fourier-processing apparatus was mounted on the other side of the slit. The lenses used in the apparatus had a focal length of 16 cm. All the most important proportions and spacings indicated in Fig. 1 were followed. An AO cell made from paratellurite was chosen as the AO filter, since a TeO_2 cell required substantially less electric energy than a $LiNbO_3$ cell and required no cooling system. A $LiNbO_3$ piezoconverter that generated a transverse acoustic wave was cemented to the (110) face of the TeO_2 crystal. The AO interaction length was 0.6 cm, and the size of the converter was 0.6 × 0.4 cm. A slow wave propagated in the crystal at 617 m/s. The optical radiation was directed at a small angle to the crystal's [001] optic axis. Anisotropic and isotropic diffraction was carried out in the crystal on the sound in this case, and this was verified from the existence of triple diffraction [8].

When the high-frequency signal voltage supplied to the converter (in this case the optimum voltage of 7.8 V), the angular orientation of the AO cell, and the 26.6 MHz sound frequency were chosen, a two-dimensional contour of the image was distinctly observed on the screen in both the zeroth and the first diffraction orders with different positions of the output polarizer P_2. Figure 5 shows photographs of the diffraction patterns of the AO fields of the zeroth order [Fig. 5(a)] and the first order [Fig. 5(b)], observed on the output screen S_{out} of the

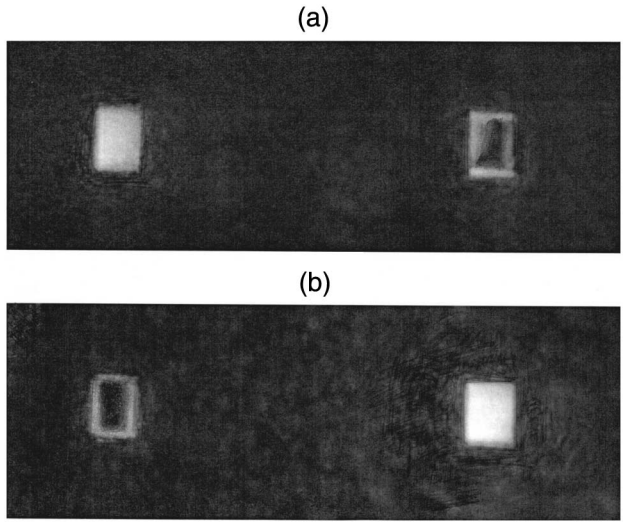

Fig. 5. Results of experimental Fourier processing of an optical image in the form of a rectangular aperture in the (a) zeroth and (b) first Bragg orders.

apparatus. The contour was clearly observed in zeroth-order diffraction when the angle of the output polarizer was $\psi = 90°$ and in first order at $\psi = 0°$. The contours are formed with fairly good quality in both the vertical and the horizontal directions. Some disagreement of the experimental data with the theoretical results (a slight difference in the sound frequencies, the angular orientation of the output polarizer, and the sound powers in theory and experiment, with the sound power in the experiment being substantially less than the theoretically predicted value, etc.) can be caused by a number of factors (inaccuracy of the model that describes a gyrotropic crystal, divergence of the sound, inaccurate orientation of the crystal faces, etc.). In any case, in the opinion of the authors of this article, the experiments completely confirmed that a two-dimensional image contour based on AO spatial-frequency filters could be obtained using the dual-mode diffraction regime.

4. CONCLUSIONS

Based on the above explanation, the following conclusions can be drawn:

A version of AO diffraction of dual-mode radiation on one acoustic wave in uniaxial crystals has been considered in which the optical radiation propagates close to the optic axis while the acoustic wave propagates orthogonally to the optic axis.

The amplitudes of all the optical waves that participate in the diffraction have been calculated, using as an example a uniaxial $LiNbO_3$ crystal and a uniaxial gyrotropic TeO_2 crystal. The transfer functions (diffraction fields) of each of these crystals have been obtained.

It has been shown that, in all cases, the fields have a region of 2° × 2° in both the zeroth and first orders of diffraction, making it possible to obtain a two-dimensional contour of the image when it is Fourier-processed. This shows that it is promising to use the corresponding AO cells as spatial-frequency filters for processing two-dimensional images.

Experiments have been carried out using AO cells made from TeO_2. Regimes have been found in which a two-dimensional contour of an image is formed in both the zeroth and first diffraction orders. A transition is made from one regime to the other by rotating the output polarizer by 90°. All the other parameters (the frequency and power of the sound, as well as the orientation of the AO cell) remain unchanged in this case.

These results substantially broaden the possibilities of using the AO interaction for optical-image processing—in particular, for discriminating a two-dimensional contour.

Funding. Russian Foundation for Basic Research (RFBR) (15-07-02312, 16-07-00064).

REFERENCES

1. B. G. Boone, *Signal Processing Using Optics: Fundamentals, Devices, Architectures, and Applications* (Oxford University, New York, 1998).
2. V. M. Kotov, G. N. Shkerdin, D. G. Shkerdin, A. I. Voronko, S. A. Tikhomirov, J. Stiens, R. Vounckx, and V. Vandermeiren, "Fourier processing of the speckle structure of the optical field formed in the process of multiphonon Bragg diffraction," J. Opt. Technol. **74**(2), 84–86 (2007) [Opt. Zh. **24**(2), 12–15 (2007)].
3. R. A. Athale, J. van der Gracht, D. W. Prather, and J. N. Mait, "Incoherent optical image processing with acousto-optic pupil-plane filtering," Appl. Opt. **34**(2), 276–280 (1995).
4. V. M. Kotov, G. N. Shkerdin, D. G. Shkerdin, and E. V. Kotov, "Image contouring in diffraction orders in the process of acousto-optic interaction," Radiotekh. Elektron. **54**(6), 747–749 (2009).
5. V. I. Balakshy, V. B. Voloshinov, T. M. Babkina, and D. E. Kostyuk, "Optical image processing by means of acousto-optic spatial filtration," J. Mod. Opt. **52**(1), 1–20 (2005).
6. V. I. Balakshiĭ, "Influence of the divergence of a light beam on the characteristics of collinear diffraction," Opt. Spectrosc. **103**(5), 804–810 (2007) [Opt. Spektrosk. **103**(5), 831–837 (2007)].
7. V. I. Balakshy and D. E. Kostyuk, "Acousto-optic image processing," Appl. Opt. **48**(7), C24–C32 (2009).
8. V. I. Balakshiĭ, V. N. Parygin, and L. E. Chirkov, *Physical Principals of Acousto-optics* (Radio i Svyaz', Moscow, 1985).
9. V. M. Kotov, *Acousto-optics: Bragg Diffraction of Multicolor Radiation* (Yanus-K, Moscow, 2016).
10. L. N. Magdich and V. Ya. Molchanov, *Acousto-optic Devices and Their Use* (Sov. Radio, Moscow, 1978).
11. V. Yu. Rakovskiĭ and A. S. Shcherbakov, "Multiphonon Bragg scattering of light by acoustic waves," Sov. Phys. Tech. Phys. **35**(7), 815 (1990) [Zh. Tekh. Fiz. **60**(7), 107–114 (1990)].
12. M. Born and E. Wolf, *Principles of Optics: Electromagnetic Theory of Propagation, Interference, and Diffraction of Light* (Pergamon Press, Oxford, 1970; Nauka, Moscow, 1973).
13. M. P. Shaskol'skaya, ed., *Acoustic Crystals* (Nauka, Moscow, 1982).
14. D. V. Sivukhin, *General Course of Physics, Vol. 4: Optics* (Fizmatlit MFTI, Moscow, 2002).
15. V. B. Voloshinov, V. N. Parygin, and L. E. Chirkov, "Some features of the anisotropy of Bragg diffraction," Vestn. Mosk. Gos. Univ. Ser. 3 Fiz., Astr. **17**(3), 305–312 (1976).